Estuaries Vol. 24, No. 3, p. 381–397 June 2001

Calculating Optical Water Quality Targets to Restore and Protect Submersed Aquatic Vegetation: Overcoming Problems in Partitioning the Diffuse Attenuation Coefficient for Photosynthetically Active Radiation

CHARLES L. GALLEGOS*

Smithsonian Environmental Research Center, P. O. Box 28, Edgewater, Maryland 20137

ABSTRACT: Submersed aquatic vegetation (SAV) is an important component of shallow water estuarine systems that has declined drastically in recent decades. SAV has particularly high light requirements, and losses of SAV have, in many cases, been attributed to increased light attenuation in the water column, frequently due to coastal eutrophication. The desire to restore these valuable habitats to their historical levels has created the need for a simple but accurate management tool for translating light requirements into water quality targets capable of supporting SAV communities. A procedure for calculating water quality targets for concentrations of chlorophyll and total suspended solids (TSS) is derived, based on representing the diffuse attenuation coefficient for photosynthetically active radiation, K_d(PAR), as a linear function of contributions due to water plus colored dissolved organic matter (CDOM), chlorophyll, and TSS. It is assumed that K_d(PAR) conforms to the Lambert-Beer law. Target concentrations are determined as the intersection of a line representing intended reduction of TSS and chlorophyll by management actions, with another line describing the dependence of TSS on chlorophyll at a constant value of K_d(PAR). The validity of applying the Lambert-Beer law to K_d(PAR) in estuarine waters was tested by comparing the performance of a linear model of K_d(PAR) with data simulated using a more realistic model of light attenuation. The linear regression model tended to underestimate K_d(PAR) at high light attenuation, resulting in erroneous predictions of target concentrations at shallow restoration depths. The errors result more from the wide spectral bandwidth of PAR, than from irrecoverable nonlinearities in the diffuse attenuation coefficient per se. In spite of the failure of the Lambert-Beer law applied to K_d(PAR), the variation of TSS with chlorophyll at constant K_d(PAR) determined by the more mechanistic attenuation model was, nevertheless, highly linear. Use of the management tool based on intersecting lines is still possible, but coefficients in the line describing the dependence of TSS on chlorophyll at constant K_d(PAR) must be determined empirically by application of an optical model suitably calibrated for the region of interest. An example application of the procedure to data from the Rhode River, Maryland, indicates that approximately 15% reduction in both TSS and chlorophyll concentrations, or 50% reduction in chlorophyll alone, will be needed to restore conditions for growth of SAV to levels that existed in the late 1960s.

Introduction

Submersed aquatic vegetation (SAV) is an important component of coastal ecosystems. It is believed that nearly 600,000 acres of SAV covered the bottom of Chesapeake Bay in historic times, but catastrophic declines occurred during the 1960s and 1970s (Orth and Moore 1983). Coverage in recent years has increased about 70% above the lowest areal coverage of 40,000 acres recorded in 1984. Because of the ecological importance of SAV, the Chesapeake Bay Program has set a goal to restore 114,000 acres of SAV throughout historically vegetated areas of the Bay by the year 2005.

The principal factor believed to limit the distribution of SAV is the availability of light at the plant surface (Duarte 1991; Dennison et al. 1993). SAV in mesohaline and polyhaline estuaries appears to require a long-term average of about 22% of surface irradiance to survive, while that in oligohaline and tidal freshwater regions appear to require c. 13% of surface irradiance (Batiuk et al. 1992; Dennison et al. 1993; Carter et al. 2000). A wide variety of methods has been used to estimate the light requirement of SAV, but the most reliable estimates generally are determined by comparing in situ depth distributions of SAV with the long-term median value of diffuse attenuation coefficient, K_d(PAR), for downwelling photosynthetically active radiation (PAR, 400 to 700 nm).

The diffuse attenuation coefficient is the empirical descriptor of the penetration of cosine-weighted downwelling irradiance underwater, i.e.,

$$E_d(Z) = E_d(0)\exp[-K_d(\mathrm{PAR})Z] \qquad (1)$$

where $E_d(Z)$ = downwelling cosine-weighted irra-

* Tele: 443/482-2240; fax: 443/482-2380; e-mail: gallegos@serc.si.edu.

diance (PAR) at depth Z, and $E_d(0)$ = downwelling cosine-weighted irradiance just beneath the air-water interface. Let Z_{max} denote the maximum depth of colonization of SAV. The 22% requirement is based on the observed tendency for the dimensionless product, $Z_{max}K_d(PAR)$, to cluster around 1.5 (Duarte 1991; Dennison et al. 1993). Of course, other factors influence the maximum depth of colonization by SAV (Koch 2001), especially light attenuation at the leaf surface by epiphytic algae and attached matrix of organic detritus and inorganic silts and clays (Twilley et al. 1985; Kemp et al. 2000). Variability in the optical density of material attached to the leaf surface may explain some of the scatter in plots of Z_{max} against percentage of incident light availability (Dennison et al. 1993). Adequate penetration of light through the water column, quantified by $K_d(PAR)$, is a necessary but not sufficient condition for colonization by SAV.

In order to take management action to restore conditions that permit growth of SAV, it is necessary to know how the value of $K_d(PAR)$ depends on the suspended and dissolved matter in the water. The diffuse attenuation coefficient is referred to as an apparent optical property (AOP), because its value depends not only on the concentrations of light attenuating components in the water, but also on the angular distribution of the underwater light field (Morel and Smith 1982). It is affected by factors in addition to water quality, e.g., surface waves, solar incidence angle, depth, and cloud cover. Optical properties that depend only on the contents of the water (i.e., that are independent of the ambient light field) are referred to as inherent optical properties (IOPs, Kirk 1994).

One goal in the field of hydrologic optics has been to determine the relationship between AOPs and IOPs (Mobley 1994). The IOPs most relevant to the problem of determining water quality concentrations suitable for restoring SAV are the absorption coefficient, *a,* and the scattering coefficient, *b.* The absorption and scattering coefficients can be expressed as the sum of contributions due to different optically active constituents, and the effect of each component is directly proportional to its concentration: i.e., IOPs are additive and linear and thus obey the Lambert-Beer law. This is not true generally of AOPs, such as $K_d(PAR)$ (Kirk 1994). Nevertheless, the need exists in the management community for a diagnostic tool able to accurately and quantitatively attribute light attenuation to the content of the water. Accuracy is needed to assure that the actions taken to improve water quality will result in sufficient reduction in light attenuation to promote expansion of SAV, while maintaining cost effectiveness by not dictating larger reductions than are actually necessary. For a diagnostic tool to be useful to managers, it needs to be accessible to non-specialists, able to batch-process extensive water quality data sets, and be usable with very limited optical data.

The simultaneous need for accuracy and ease of use presents potentially conflicting requirements. Models believed to faithfully represent the processes of radiative transfer underwater are written for monochromatic light [i.e., a complete spectrum must be simulated to determine $K_d(PAR)$] and require specification of *a, b,* (functions of wavelength), and the scattering phase function (Mobley et al. 1993). Although extremely useful for research problems, such as generating empirical relationships between IOPs and AOPs (Kirk 1984), such models are still too complex for use in the water quality management community. At the other extreme, some researchers have applied the Lambert-Beer law to the diffuse attenuation coefficient by modeling $K_d(PAR)$ as a linear function of water quality concentrations (Lorenzen 1972; Smith 1982; Verduin 1982; Stefan et al. 1983). Linear representation of $K_d(PAR)$ may meet the ease-of-use criteria, but the inherent inaccuracies in doing so are as yet unquantified (c.f., Kirk 1994).

Gordon (1989) used a Monte Carlo model of an ocean-atmosphere system to examine the severity of violation of the Lambert-Beer law by narrow waveband spectral irradiance in Case 1 waters, i.e., waters in which the optical properties are governed by phytoplankton pigments and their detrital degradation products. He demonstrated that the diffuse attenuation coefficient for narrow-band irradiance obeyed the Lambert-Beer law to a high degree of accuracy in Case 1 waters, provided the measurements were divided by an easily calculated distribution coefficient that corrects for the effects of variation in sun angle, the relative proportion of diffuse sky irradiance, and sea state. Extension to Case 2 waters (in which the optical properties are substantially affected by colored dissolved organic matter (CDOM) and non-algal particulate matter) did not significantly increase errors as long as waters with high concentrations of non-absorbing particles were avoided (Gordon 1989). To apply the Lambert-Beer law to $K_d(PAR)$ in situations useful for setting water quality management goals requires extension of the law to broadband irradiance, and application in waters with high concentrations of terrigenous suspended solids. The errors incurred by doing so require further examination.

In this paper I use a series of models of decreasing complexity and increasing ease of use to examine the severity of systematic errors incurred by applying the Lambert-Beer law to $K_d(PAR)$, particularly as they relate to the determination of water

quality targets for restoring SAV. After a brief review of optical models, I validate the performance of the spreadsheet-based model of Gallegos (1994) against a more realistic Monte Carlo model of radiative transfer (Kirk 1989), and use the spreadsheet model to generate pseudo-data for estimation of a linear regression model. Analysis of the linear regression representation indicates that a single regression is prone to errors when used across a broad range of water quality concentrations. Improvements can be made by using separate regressions for different target restoration depths, provided information about spectral specific-absorption and scattering coefficients in the different ranges is available.

Model Descriptions

Complete description of the equation of radiative transfer and the models that solve it is beyond the scope of this paper. It is still useful to review the processes that attenuate light underwater to better appreciate the divergence of the different modeling approaches that have been taken, although rigorous explanations are given in several recent sources (Davies-Colley et al. 1993; Kirk 1994; Mobley 1994).

The equation of radiative transfer describes a photon budget for monochromatic light within an incremental solid angle (see, e.g., Fig. 1.6 in Kirk 1994). Photons traveling in a given direction are lost by absorption and by being scattered in a different direction. Gains of photons within a solid angle are due to scattering of photons that occurs from all other directions into the solid angle being considered. The scattering phase function, which describes the probability distribution of scattering angles, is needed to account for the fate of scattered photons. Integration of the equation for an incremental solid angle over all directions in 3 dimensions accounts for all losses of photons as depth increases.

Mobley et al. (1993) compared different methods of solving the radiative transfer equations and found that 7 different models provided consistent predictions of irradiances, with Monte Carlo methods suffering somewhat from statistical fluctuations in calculated quantities at great optical depth, due to the small number of surviving photons. Errors at great optical depth are not of concern in this work, because of the emphasis here on attenuation to the 22%, or at most, the 13% penetration depth.

Monte Carlo models of the radiative transfer equation have the advantage that they are easy to program, and the procedure is, in some respects, analogous to the natural process of attenuation (Kirk 1994). The processes of absorption and scattering, which contribute to the attenuation of light, are stochastic events that occur as a result of encounters between photons and absorbing and scattering substances in the water. The values of the absorption and scattering coefficients are measures of the probability per unit distance of absorption and scattering events. Similarly, the scattering phase function describes the probability distribution of relative scattering angle, given that a scattering event has occurred.

In a series of papers, Kirk (1981, 1984, 1989) has used Monte Carlo modeling of the radiative transfer equation to estimate approximate algebraic expressions relating various AOPs but especially diffuse attenuation coefficient, to the IOPs, a and b. One expression that is particularly useful because of its simplicity and accuracy is

$$K_d = \frac{1}{\mu_0}[a^2 + G(\mu_0)\,ab]^{1/2} \qquad (2)$$

where μ_0 is the cosine of the solar zenith angle, after accounting for refraction at the (assumed flat) air-water interface, and $G(\mu_0)$ $(= g_1\mu_0 - g_2)$ is a linear function that determines the relative effect of scattering on the total rate of attenuation. Although entirely empirical, Eq. 2 is both highly accurate and very general, applying over a wide range both of solar incidence angles and of b:a ratios (Kirk 1984, 1994).

As indicated above, a and b are functions of wavelength, which complicates calculation of K_d(PAR) using Eq. 2. Absorption spectra of certain substances, such as CDOM, have simple spectral shapes that can be described by a simple negative exponential; but the absorption spectra of water and of phytoplankton pigments are irregularly shaped and are most conveniently expressed as tabulated values. There is, therefore, no closed form integration of Eq. 2 over the PAR waveband to calculate averaged K_d(PAR).

Gallegos (1994) calculated K_d(PAR) by first predicting the spectrum of diffuse attenuation coefficient, $K_d(\lambda)$. This was done by multiplying concentrations of optical water quality parameters by their experimentally determined specific-absorption and specific-scattering spectra to estimate $a(\lambda)$ and $b(\lambda)$, which were then substituted into Eq. 2. Then by propagating the incident solar spectrum to a reference depth, Z, according to Eq. 1 and numerically integrating over wavelength, K_d(PAR) was calculated as

$$K_d(\mathrm{PAR}) = -\frac{1}{Z}\ln\left[\frac{\mathrm{PAR}(Z)}{\mathrm{PAR}(0)}\right] \qquad (3)$$

The procedure is simple, fast, and easily adapted to studying the relationship of K_d(PAR) to variations in optical water quality parameters, but its

accuracy compared with mechanistic models of radiative transfer has not been determined. I refer to this simplified computational procedure as the spectrally integrated algebraic summary (SIAS) model.

At the lowest level of mechanistic realism is linear partitioning of the diffuse attenuation coefficient for PAR (Lorenzen 1972; Smith 1982; Verduin 1982; Stefan et al. 1983). Such a representation might be written

$$K_d(PAR) = K_w + k_y[CDOM] + k_c[Chl] + k_s[TSS] \quad (4)$$

where K_w = the (supposed) attenuation due to water alone, and k_y, k_c, and k_s are, respectively, specific-attenuation coefficients (i.e., attenuation per unit concentration) of CDOM, chlorophyll, and total suspended solids (TSS). Equation 4 is a statement of the Lambert-Beer law applied to $K_d(PAR)$.

Linear partitioning of $K_d(PAR)$ into contributions due to discrete factors treats the diffuse attenuation coefficient as if it were an IOP, which it is not (Kirk 1994). Doing so has several distinct advantages for management purposes. If coefficients in Eq. 4 can be specified, then the percentage contribution of each water quality constituent to the total attenuation can be calculated simply; that is, the percent attenuation due to, e.g., chlorophyll is given by $100 \cdot k_c[Chl]/\{K_w + k_c[Chl] + k_y[CDOM] + k_s[TSS]\}$. Computations to this effect can help managers rank the importance of reducing the different attenuating components.

A second advantage of applying the Lambert-Beer law to $K_d(PAR)$ is that it becomes possible to obtain analytical expressions for combinations of water quality concentrations that will result in a particular value of $K_d(PAR)$ that permits survival of SAV to a particular depth strata (Gallegos and Moore 2000). For ease of graphical presentation in 2 dimensions, I assume that one component, in this case CDOM, is relatively minor and invariant compared with the other 2 parameters, and that its effect can be combined with that of water to yield a lumped parameter, $K_{(W+CDOM)}$. The procedure is fully generalizable to 3 dimensions (e.g., Gallegos and Kenworthy 1996), and CDOM need not be ignored in locations where it comprises an important contribution to attenuation. Let f_{lr} = the light requirement for SAV growth and survival expressed as a fraction of surface incident light (i.e., 0.22 for mesohaline and polyhaline species, and 0.13 for oligohaline and tidal freshwater communities, Carter et al. 2000); and let Z_{max} = the target protection or restoration depth for SAV. Then combining Eqs. 1 and 4, we can write

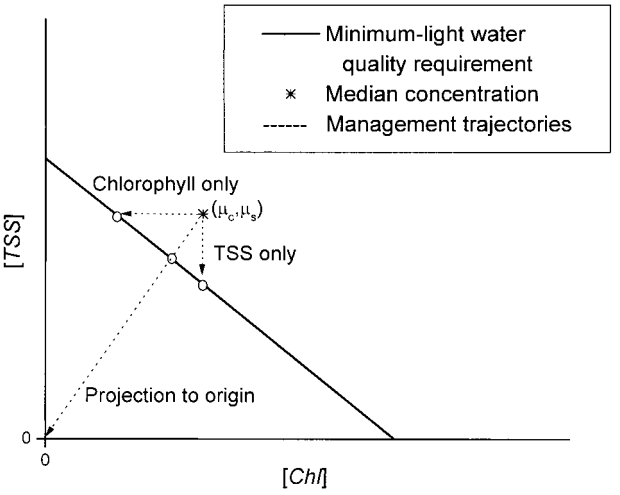

Fig. 1. Illustration of a procedure for calculating water quality targets for protection and restoration of SAV habitats. Target (open circles) concentrations relative to current median conditions (asterisk) are given as the intersection of lines defining the minimum-light water quality requirement (bold line, Eq. 6) and one of 3 management trajectories (dotted arrows, Eq. 7).

$$\frac{-\ln(f_{lr})}{Z_{max}} = K_{(W+DOC)} + k_c[Chl] + k_s[TSS] \quad (5)$$

Equation 5 can be rearranged to express linear combinations of [Chl] and [TSS] that just meet the f_{lr} requirement,

$$[TSS] = \frac{-\ln(f_{lr}) - Z_{max}K_{(W+CDOM)}}{k_s Z_{max}} - \frac{k_c}{k_s}[Chl] \quad (6)$$

which defines a line with slope = $-k_c/k_s$, and [Chl] = 0 intercept of $[-\ln(f_{lr}) - Z_{max}K_{(W+CDOM)}]/k_sZ_{max}$. Equation 6 thus defines a linear minimum-light habitat requirement for SAV based on the Lambert-Beer law.

The use of Eq. 6 for setting target water quality goals is illustrated schematically in Fig. 1. If the long-term median concentrations of chlorophyll and TSS fall outside the triangular region enclosed by the axes and Eq. 6 (i.e., the minimum-light water quality requirement), then chlorophyll and/or TSS must be reduced. Target concentrations can be determined analytically by solving for the intersection of 2 lines. Three ways of determining target concentrations are illustrated in Fig. 1. Let the point defined by the existing long-term median concentrations of chlorophyll and TSS be denoted (μ_c, μ_s). Lines defining reduction strategies involving, respectively, reducing chlorophyll only, reducing TSS only, and reducing both chlorophyll and TSS are given by

TABLE 1. Formulae for coordinates of target concentrations of chlorophyll, [Chl], and suspended particulate matter, [SPM], determined by intersection of Eq. 6 with Eq. 7a–c. Last column gives conditions for obtaining a positive concentration as the intersection.

$$\xi = \frac{-\ln(f_{lr}) - Z_{max}\,K_{(W+CDOM)}}{Z_{max}}$$; other symbols defined in text.

Management Action	[Chl]	[SPM]	Condition
Chlorophyll reduction only	$\frac{\xi - k_s\mu_s}{k_c}$	μ_s	$\mu_s \le \frac{\xi}{k_s}$
SPM reduction only	μ_c	$\frac{\xi - k_c[Chl]}{k_s}$	$\mu_c \le \frac{\xi}{k_c}$
Projection to origin	$\frac{\mu_c\xi}{(k_s\mu_s + k_c\mu_c)}$	$\frac{\mu_s\xi}{(k_s\mu_s + k_c\mu_c)}$	No restriction
Normal projection	$\frac{k_c\xi}{k_s^2 + k_c^2}$	$\frac{k_s\xi}{k_s^2 + k_c^2}$	$\mu_s \le \frac{k_s}{k_c}\mu_c + \frac{\xi}{k_s}$ and $\mu_s \ge \frac{k_s}{k_c}(\mu_c - \frac{\xi}{k_c})$

$$[TSS] = \mu_s \quad (7a)$$

$$[Chl] = \mu_c \quad (7b)$$

$$[TSS] = \frac{\mu_s}{\mu_c}[Chl] \quad (7c)$$

A fourth reduction strategy (not shown in Fig. 1) can be defined which is normal to Eq. 6. The normal line has a slope = k_s/k_c and passes through point (μ_c, μ_s); it represents the shortest distance in chlorophyll-TSS space from current conditions to the minimum-light water quality requirement. Coordinates defining the target concentrations determined by the intersections of Eq. 6 with Eq. 7a–c are given in Table 1.

Such simplifications are useful for prioritizing management efforts, provided the calculations are reliable. In view of the known violation of the assumption of linearity for AOPs, the degree of reliability of this assumption needs to be established. I examine the magnitude of errors incurred by violation of the assumption of linearity after validating the SIAS model based on Eq. 2 (Gallegos 1994) against Monte Carlo modeling of the radiative transfer equation.

Description of Data and Modifications to SIAS Model

The model of Gallegos (1994) requires specific-absorption spectra of chlorophyll, CDOM, and TSS, as well as the specific-scattering coefficient of TSS. Gallegos (1994) used turbidity as the measure of scattering coefficient, and absorption coefficient at 440 nm measured in a spectrophotometer on 0.2-μm filtrate (i.e., g_{440}) as a measure of CDOM. The version of the model used in this work was modified to make it amenable to the water quality data available from the Chesapeake Bay Water Quality Monitoring Program (U.S. Environmental Protection Agency, www.chesapeakebay.net/data/). Their monitoring data include chlorophyll, dissolved organic carbon (DOC), and total and fixed suspended solids, but not turbidity. Therefore it was necessary to modify the functions that parameterize absorption by CDOM, absorption by non-algal particulate matter, and scattering by suspended solids.

For lack of a more suitable measure of CDOM in the Chesapeake Bay Water Quality Monitoring Program, a modification of Eq. 5 in Gallegos et al. (1990) was used to calculate g_{440} from measurements of DOC: $g_{440} = 0.167[DOC]$. To express absorption by non-algal particulate matter in terms of TSS, 34 absorption spectra of particulate matter captured on GF/F glass fiber filters and extracted in methanol to remove phytoplankton pigments were normalized to the concentration of TSS. These were individually fit to the function

$$\frac{a_d(\lambda)}{TSS} = \sigma_{400}\exp[-s_d(\lambda - 400)] + \sigma_{bl} \quad (8)$$

where $a_d(\lambda)$ = spectral absorption by non-algal particulate matter, σ_{bl} = the long-wave specific-absorption coefficient, σ_{400} scales the absorption amplitude at short wavelengths, and s_d determines the rate of exponential decrease to σ_{bl}. In Eq. 8, $a_d(\lambda)$ and TSS are measurements, and σ_{400}, s_d, and σ_{bl} are estimated parameters. Mean values of the estimated parameters, σ_{400}, s_d, and σ_{bl}, are given in Table 2, along with estimates of the variability observed.

Parameterization of scattering coefficient in terms of TSS is based on the observation that scattering coefficient frequently scales with turbidity measured in (NTU) with a constant near unity (Kirk 1980; Weidemann and Bannister 1986; Vant

TABLE 2. Means, standard deviations, minima, and maxima of parameters describing absorption by non-algal particulate matter (Eq. 8) in the Rhode River, Maryland. Statistics are based on 34 water samples filtered onto GF/F filter and scanned in an integrating sphere interfaced to an EG&G Gamma spectral radiometer.

	σ_{400} ($m^2\ g^{-1}$)	σ_{bl} ($m^2\ g^{-1}$)	s_d (nm^{-1})
Mean	0.24	0.0305	0.0164
Standard deviation	0.11	0.0133	0.0021
Minimum	0.096	0.0098	0.0124
Maximum	0.31	0.0621	0.0196

1990). A regression analysis of turbidity against TSS using data from the Rhode River and Chincoteague Bay (Gallegos unpublished) was used to estimate scattering coefficient, from TSS (Fig. 2a). The modified treatment represents scattering as

$$b(\lambda) = 0.32[TSS]\left(\frac{550}{\lambda}\right) \quad (9)$$

where the $550/\lambda$ term introduces the inverse wavelength dependence suggested by Morel and Gentili (1991).

In order to use the SIAS model of Gallegos (1994) with TSS as one of the optical water quality input parameters, it is important to examine the interrelationships between TSS and other inputs, so that unrealizable combinations of the 2 are not used as inputs in the model. This is especially true for chlorophyll, which is itself part of the suspended particulate matter. Total suspended solids consist of the dry weight of all particulate matter in a sample, including clay, silt, and sand mineral particles, living phytoplankton and heterotrophic plankton, and particulate organic detritus. Currently it is difficult to distinguish optically the effects of mineral and non-algal particulate matter, in part due to insufficient attention paid to optical effects of inorganic particulate matter (Mobley 1994). The similar relationships between turbidity (scattering) and TSS in Fig. 2a occurs despite a much greater contribution of phytoplankton to the suspended material in the Rhode River compared with Chincoteague Bay (Fig. 2b). Phytoplankton contribute to scattering on a dry weight basis about the same as inorganic suspended solids and organic detritus. The generality of these observations is uncertain. It is likely that relationships as precise as these would be difficult to obtain if the geographic extent or length of time covered were increased, and different instruments and standards were employed.

As noted above, phytoplankton are part of the suspended particulate load of any water sample. TSS and chlorophyll cannot be independent because phytoplankton contribute to the particulate

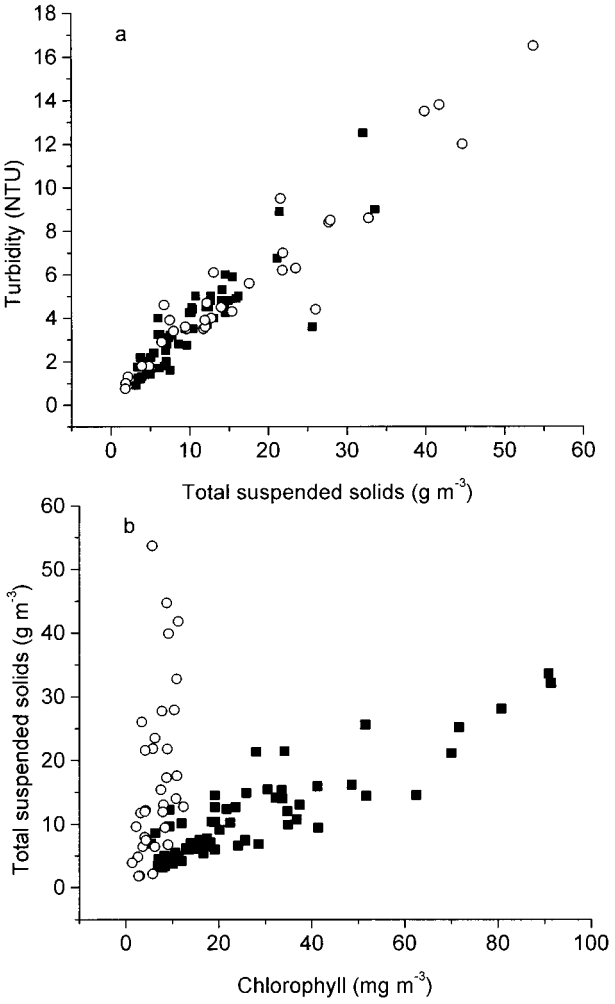

Fig. 2. a) Relationship between turbidity (a surrogate for scattering coefficient) and total suspended solids concentration in Chincoteague Bay, Maryland (open circles) and the Rhode River, Maryland (filled squares). b) Relationship between total suspended solids and chlorophyll.

organic matter in a sample. Upon combustion, all organic matter in a sample is oxidized, leaving behind the mineral component and ash of the organic fraction. The fraction remaining after combustion is referred to as fixed suspended solids (FSS), and the difference TSS-FSS is called total volatile suspended solids (TVSS).

FSS and TVSS along with particulate organic carbon (POC) have been measured at the Virginia tidal tributary and mainstem stations of the Chesapeake Bay Water Quality Monitoring Program. The relationship between TVSS and POC is very noisy (Fig. 3a), but on average, POC is about 30% of TVSS. This estimate is within expected limits, being larger than that of living phytoplankton (26%, Sverdrup et al. 1942) and lower than that of carbohydrate (37%). Because so much of POC

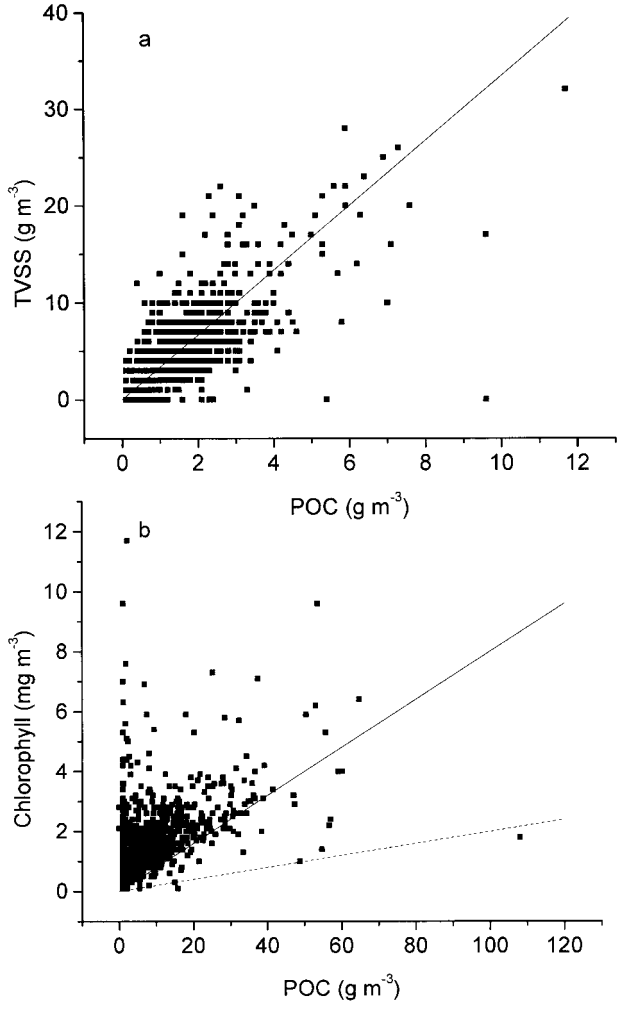

Fig. 3. a) Concentration of total volatile suspended solids (TVSS) plotted against particulate organic carbon (POC) for Virginia tidal tributary stations, 1984–1996. Line shows estimate of TVSS as POC/0.3. b) Relationship of POC to chlorophyll concentration for Virginia tidal tributary stations. Lines bracket approximate contribution of phytoplankton chlorophyll to POC based on a range of phytoplankton carbon-to-chlorophyll ratios from (dashed line) 20 to (solid line) 80 mg C (mg chl)$^{-1}$.

is heterotrophic and detrital, it is expected that a plot of POC against phytoplankton chlorophyll will display considerable scatter (Fig. 3b), but that during sudden phytoplankton blooms, phytoplankton might comprise the major component of carbon in a sample. Carbon-to-chlorophyll ratios vary widely in phytoplankton; a line with a slope ranging from about 20 to 80 mg C (mg chl *a*)$^{-1}$ provides a lower bound of most of the points in Fig. 3b, a range well within physiological limits (Geider 1987). Choosing 40 mg C (mg chl *a*)$^{-1}$ (the geometric mean of 20 and 80) as a representative C:chlorophyll ratio, and using the 30% POC:TVSS ratio of Fig. 2a, the minimum contribution of phytoplankton chlorophyll to TSS can be estimated as 0.04[Chl]/0.3, where the 0.04 results from the conversion of μg to mg chl l^{-1}. Thus, the line defined by [TSS] = 0.04[Chl]/0.3 will generally be a lower bound for most observations of chlorophyll and TSS, consisting of instances when phytoplankton comprise nearly all of the suspended particulate matter.

When using the modified model with simulated input water quality parameters, the value of TSS used in Eqs. 5 and 6 is generated from assumed independent contributions due to FSS, non-algal volatile suspended solids, and a phytoplankton component given as above. A single set of coefficients in Eqs. 5 and 6 is used to account for the optical effect of each component, though the possibility exists to treat them separately, when information on the specific-absorption and scattering spectra of each component becomes available.

Note also that inclusion of phytoplankton chlorophyll in the suspended particulate matter means that reduction in chlorophyll by management action entails a proportionate reduction in TSS by at least the amount of the dry weight of phytoplankton, estimated above as 0.04[Chl]/0.3. The modification to target concentrations produced by inclusion of this effect is given by Gallegos and Moore (2000).

Results and Discussion

Validation of the SIAS Model

The Monte Carlo model used to solve the radiative transfer equations in this work was the nonspectral version used by Kirk (1989). Minor modifications were made to allow simple input of optical properties specific to the analyses undertaken in this work. I tested my implementation of the model by attempting to reproduce Kirk's (1984) values for the coefficients g_1 and g_2 (see definition of terms in Eq. 2) for the penetration of light from the surface to the 1% light level. I conducted 432 runs of the model, allowing *a* to vary from 0.5 to 4 m^{-1}, and *b* to vary from 0.5 to 40 m^{-1}, encompassing a range of *b*:*a* ratios from 0.5 to 20. Using least squares estimation, I found $g_1 = 0.430$ and $g_2 = 0.194$ compared with Kirk's values of 0.425 and 0.190, respectively. $G(\mu_0)$ plotted against μ_0 for the 2 sets of coefficients were virtually indistinguishable from one another (data not shown), and therefore my implementation of the computer code appears equivalent to Kirk's (1984).

I then used the modified SIAS model to calculate simulated absorption and scattering spectra from 400 to 700 nm at 5-nm intervals for 6 widely differing water types for use in the Monte Carlo model of Kirk (1989). The assumed water quality

TABLE 3. Assumed water quality concentrations used to simulate 6 absorption and scattering spectra for comparing spreadsheet model with Monte Carlo model of radiative transport. DOC = dissolved organic carbon; Chl = chlorophyll *a*, TSS = total suspended solids, FSS = fixed suspended solids, and HDPOC = heterotrophic and detrital particulate organic carbon. TSS was calculated by equation:

$$\mathrm{TSS} = \mathrm{FSS} + \frac{0.04[\mathrm{Chl}] + \mathrm{HDPOC}}{0.3}.$$

Water Type	Depth (m)	DOC (mg l^{-1})	Chl (mg m^{-3})	TSS (mg l^{-1})	FSS (mg l^{-1})	HDPOC (mg l^{-1})
Clear coastal	7	1.75	4	4.87	3.5	0.25
Average estuarine	5	2	10	9.67	5	1
Turbid	2	3	12	48.27	40	2
Eutrophic	2	3	90	18.33	3	1
CDOM stained	2	$g_{440} = 8\ m^{-1}$*	4	4.87	3.5	0.25
Non-absorbing particles	2	0	0	20**	20	0

* Model was modified for CDOM-stained simulation to calculate absorption by CDOM directly from absorption coefficient of dissolved matter at 440 nm.

** Specific scattering at 550 nm was changed from 0.31 to 0.5 $m^2\ g^{-1}$ and specific absorption coefficient set to 0 at all wavelengths to simulate non-absorbing, highly scattering particles.

conditions are given in Table 3, and the simulated diffuse attenuation spectra are shown in Fig. 4a. Scattering spectra were simulated according to Eq. 8 using values of TSS given in Table 3. For each simulated water type a Monte Carlo simulation with each of 61 combinations of absorption and scattering coefficient was performed, covering the visible spectrum from 400 to 700 nm in 5-nm increments. From these, reference spectral diffuse attenuation coefficients, $K_d(\lambda)$, were calculated from the log-linear decrease in number of photons with depth. These were compared with values calculated in the SIAS model according to Eq. 2. The number of photons remaining at the bottom of the water column (corrected for the cosine of the direction of propagation) was summed, and the log-transformed sum was used to calculate the average $\{K_d(\mathrm{PAR})\}$ over the water column as $\{K_d(\mathrm{PAR})\} = -(1/Z)\ln(\#\ \text{of photons remaining}/\#\ \text{of photons introduced})$, analogous to Eq. 3 (Fig. 4b). These reference $\{K_d(\mathrm{PAR})\}$ values were compared with values calculated in the SIAS model after numerical integration of the spectrum and application of Eq. 3.

Both $K_d(\lambda)$ calculated in the SIAS model and $\{K_d(\mathrm{PAR})\}$ calculated by numerical integration agreed very well with the reference values calculated by full Monte Carlo simulation of the radiative transfer equations (Fig. 4b). This degree of agreement is a direct result of the empirical accuracy of Eq. 2 in summarizing the outcome of the radiative transfer process. In the SIAS model, none of the information about the angular distribution of the underwater light field is retained, as it is with the Monte Carlo simulation. Nevertheless, Fig. 4b indicates that the SIAS model is an accurate tool for translating information on concentrations of optical water quality parameters into estimates of fraction of irradiance penetrating to particular depths of interest. The principal limitation in such predictions is, therefore, the accuracy of the specific-absorption and scattering spectra, and not the simplifications inherent in the use of Eq. 2 and numerical integration over wavelength to calculate $K_d(\mathrm{PAR})$ from *a* and *b*.

Assessment of Nonlinearity in $K_d(\mathrm{PAR})$

Gordon (1989) demonstrated that, after applying a simple factor to correct for solar incidence angle, diffuse sky irradiance, and surface waves, narrow-band $K_d(\lambda)$ obeys the Lambert-Beer law in Case 1 waters to a high degree of accuracy. To what extent can the same be said of broadband $K_d(\mathrm{PAR})$, particularly in Case 2 waters? I addressed this question by using the spreadsheet implementation of Eqs. 2 and 3 together with a software package (Crystal Ball) that permits assignment of random distributions to values in spreadsheets, in this case, the concentrations of DOC, chlorophyll, and TSS. This procedure generated pseudo data for assessment of nonlinearity, with the only error in simulated K_d being that expected on the basis of Fig. 4b. Input distributions for the water quality data were based on an analysis of data from the Chesapeake Bay Water Quality Monitoring Program, their station 3.3C (Fig. 5). This station is in the mesohaline zone and is the closest mainstem station to the Rhode River, Maryland, the location where the optical model of Gallegos (1994) was calibrated. This procedure produced a close match between simulated and observed water quality distributions (Fig. 5a–c) as well as the dependent variable, $K_d(\mathrm{PAR})$ (Fig. 5d). The simulated water quality input values therefore represent a realistic Case 2 scenario, and the simulated K_d contain the full nonlinear dependence inherent in Eqs. 2 and 3,

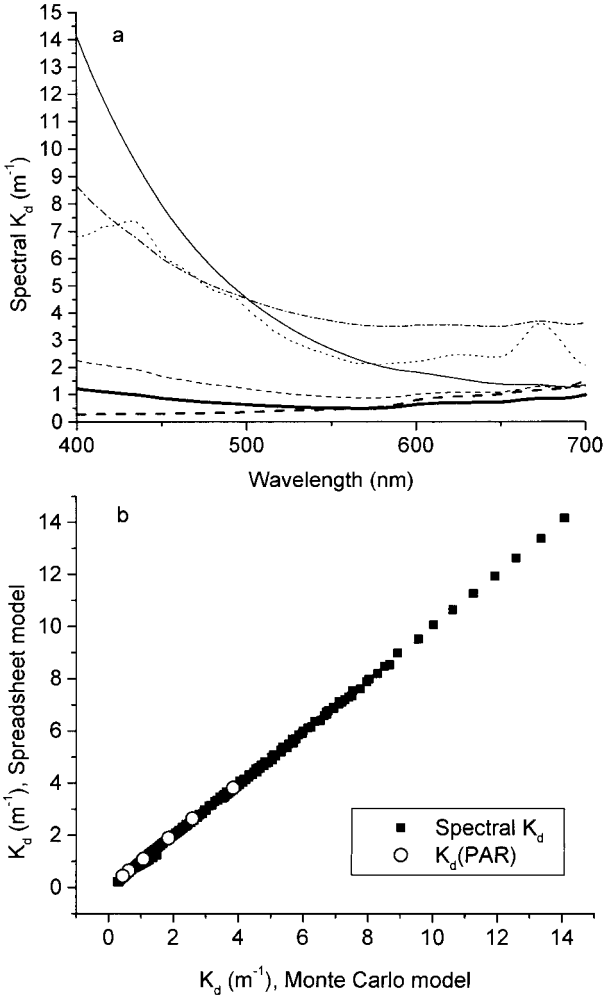

Fig. 4. a) Simulated spectra of diffuse attenuation coefficient associated with water types with water quality conditions given in Table 3: bold solid line = clear coastal waters; bold dashed line = non-absorbing particles; thin dashed line = average estuarine; dotted = eutrophic; dot-dashed = turbid; thin solid = CDOM dominated. b) Values of spectral diffuse attenuation coefficient (squares) and K_d(PAR) (circles) calculated by modified spreadsheet model compared with full simulation of the radiative transport equations by Monte Carlo model.

without variability due to imprecise measurements or to changing optical properties.

To assess nonlinearity I evaluated the regression of K_d against simulated concentrations of DOC, chlorophyll, and TSS, examined the dependence of specific-attenuation coefficients on input water quality concentrations, and quantified the magnitude of errors in estimated target water quality concentrations. We can isolate issues relating to application of the Lambert-Beer law to K_d in Case 2 waters from those involving application of the law to broadband irradiance (PAR) by separately evaluating nonlinearity in narrow band $K_d(\lambda)$ and in K_d(PAR).

I chose 555 nm as the wavelength for comparing narrow band K_d with K_d(PAR) because, in Case 2 waters, the minimum attenuation occurs in the green portion of the spectrum. This results from the competing effects of absorption by CDOM and by TSS in the blue, and by chlorophyll and water itself in the red regions of the spectrum. $K_d(555)$ therefore tends to be lower than K_d(PAR), but is nevertheless a close approximation of K_d(PAR) in these simulations (Fig. 6) and is a suitable wavelength for isolating the effects of Case 2 water quality conditions from those due to consideration of broadband (i.e., PAR) irradiance.

The correction for the geometry of the underwater light field employed by Gordon (1989) included terms for the angle of incidence of the direct solar beam, the relative proportion of diffuse sky versus direct sun irradiance, and wind-driven gravity waves. Because the Monte Carlo model of Kirk (1984) and the algebraic summary equations derived from it (Eq. 2) do not include diffuse sky irradiance or the effects of surface waves, Gordon's (1989) correction factor for the diffuse attenuation coefficients simulated in this work reduces to correction for the angle of incidence of the direct solar beam, and is equivalent to multiplication of K_d by the cosine of the refracted solar incidence angle, μ_0. The utility of this correction factor to restore linearity between simulated diffuse attenuation coefficients and water quality concentrations was determined for both narrow and broadband irradiance.

Performance of the Regression

Coefficients of determinations of linear regressions between simulated diffuse attenuation coefficients (with and without correction for solar incidence angle) and water quality concentrations varied from c. 0.96 to > 0.99 (Table 4). The r^2 was lowest for K_d(PAR) uncorrected for solar incidence angle, and highest for $\mu_0 K_d(555)$. Multiplication by μ_0 was effective at reducing the standard errors of the regression to about half their values without correction (Table 4). The standard errors of the regression are about 6% of the simulated mean for K_d, and about 3–4% of the simulated means for $\mu_0 K_d$.

Residuals of the regressions increased in magnitude as a function of the simulated value for both narrow band $K_d(555)$ and broadband K_d(PAR) (Fig. 7). Positive and negative residuals were fairly symmetrically distributed throughout the simulated range for narrow band irradiance (Fig. 7a,b). Correction for solar incidence angle reduced the magnitude of maximal residuals from about 14%

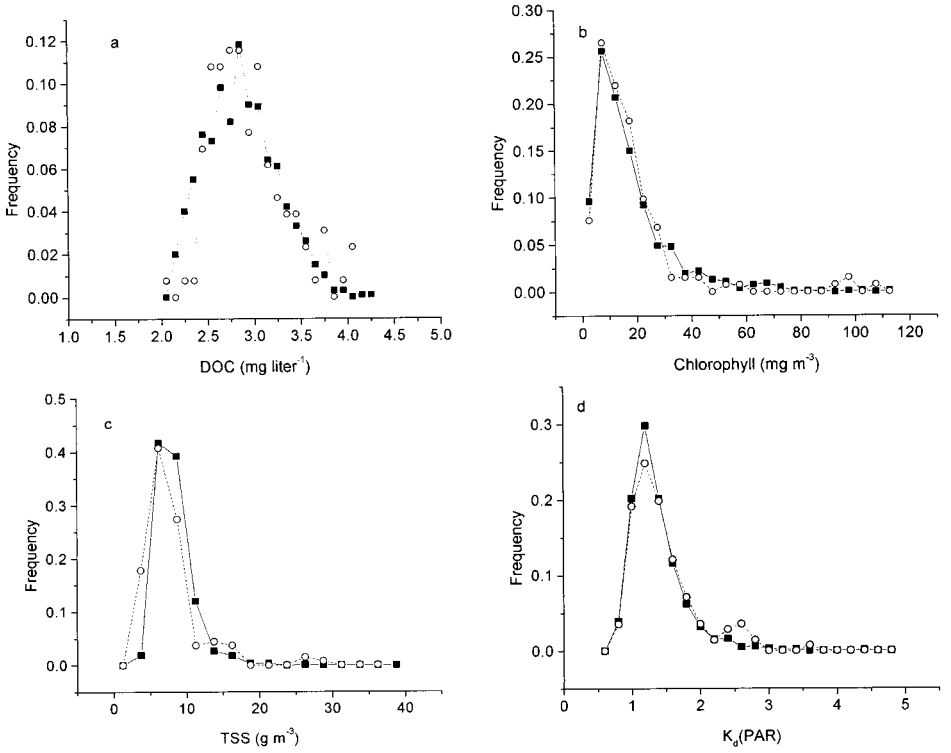

Fig. 5. Distributions of simulated (squares, solid line) and observed (circles, dashed line) water quality variables at Chesapeake Bay mainstem station 3.3C: a) dissolved organic carbon (DOC); b) chlorophyll *a*; c) total suspended solids (TSS); and d) K_d(PAR). Simulated DOC, chlorophyll, and TSS were used as inputs to the spreadsheet model, and K_d(PAR) is the output.

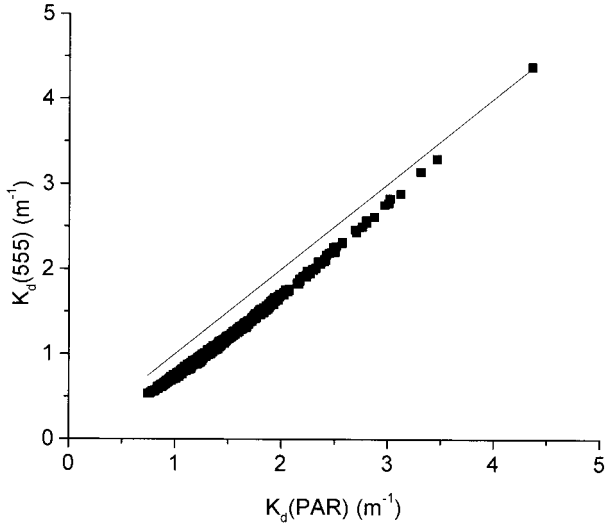

Fig. 6. Plot of simulated values of diffuse attenuation coefficient (squares) for narrow-band irradiance at 555 nm, [K_d(555)], against simulated diffuse attenuation coefficient for broadband irradiance, K_d(PAR); solid line = line of equality. The close correspondence between the two indicate that 555 nm is a suitable wavelength for isolating effects of broadband versus narrow band irradiance from those relating to Case 2 waters on violation of the Lambert-Beer law.

of simulated values (Fig. 7a) to about 8% (Fig. 7b). The magnitude of maximal residuals was similar between narrow band and broadband K_d (cf., Fig. 7a,c). Correction of broadband K_d for solar incidence angle produced a smaller reduction in magnitude of residuals than for narrow band irradiance (cf., Fig. 7c,d). Some positive correlation between residual and simulated values was present in all regressions, though it was substantially reduced by correction for solar incidence angle, and more so for K_d(PAR) than for K_d(555).

TABLE 4. Regression statistics for linear regressions of simulated diffuse attenuation coefficients for narrow band, K_d(555), and broadband, K_d(PAR), against water quality concentrations. Data were simulated using spreadsheet model with water quality concentrations drawn from random distributions given in Fig. 5. Definitions of symbols given in text. Units: K_W = m^{-1}; k_y = m^2 (g DOC)$^{-1}$; k_c = m^2 (mg chl *a*)$^{-1}$; k_s = m^2 (g TSS)$^{-1}$. r^2 (dimensionless) is the coefficient of determination; SE (m^{-1}) is the standard error of regression; and μ_0 (dimensionless) is the cosine (relative to zenith) of refracted solar incidence angle.

Dependent Variable	K_W	k_y	k_c	k_s	r^2	SE
K_d(555)	0.0796	0.0554	0.0121	0.0795	0.9745	0.0574
$\mu_0 K_d$(555)	0.0665	0.0461	0.0103	0.0621	0.9911	0.0275
K_d(PAR)	0.3315	0.0507	0.0122	0.0778	0.9617	0.0725
$\mu_0 K_d$(PAR)	0.2693	0.0429	0.0105	0.0644	0.9815	0.0408

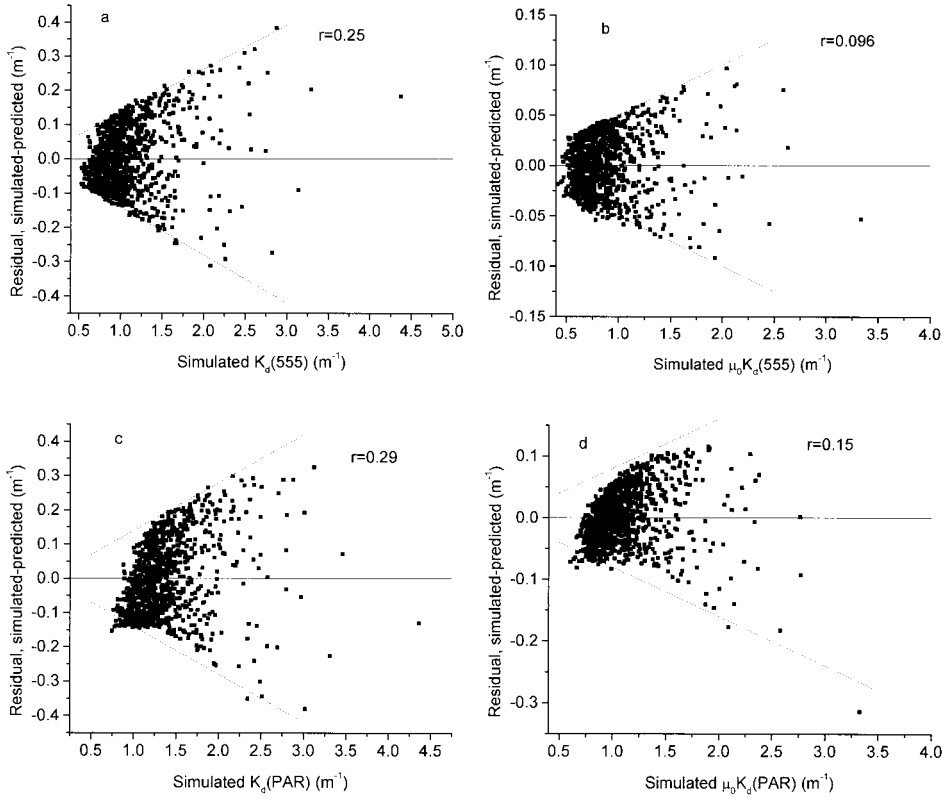

Fig. 7. Residuals of diffuse attenuation coefficient predicted by linear regression plotted against simulated value: (a) narrow band irradiance (555 nm); (b) narrow band irradiance, corrected for solar incidence angle; (c) broadband irradiance, PAR; and (d) broadband irradiance, corrected for solar incidence angle. Dotted reference lines are 14% of simulated value in (a) and (c), and 8% in (b) and (d). r is the correlation coefficient between residual and simulated value. Coefficients of regressions are given in Table 4.

Data Dependence of Specific-Attenuation Coefficients

Keeping in mind that the simulations are free of observational errors and that the optical properties of CDOM, phytoplankton, and TSS are assumed to be invariant, the specific-attenuation coefficients, calculated as above (Table 4) by linear regression of simulated K_d against water quality concentrations would be the same for any simulated set of data if the process were truly linear. The dependence of calculated specific-attenuation coefficients on the particular range of water quality concentrations used in the simulation gives one indication of the severity of potential errors incurred by wrongly applying the Lambert-Beer law to K_d.

Specific-attenuation coefficients were determined from data simulated to match water quality conditions along a north-to-south transect in mainstem Chesapeake Bay (Fig. 8). Water quality data were obtained from the Chesapeake Bay Program website, http://www.chesapeakebay.net/data/. Concentrations of DOC differed only slightly among stations (Fig. 8a), whereas distributions of chlorophyll (Fig. 8b) and TSS (Fig. 8c) showed marked differences that might be capable of affecting regression coefficients of K_d against water quality concentrations. Water quality at the northernmost station, CB2.2, is dominated by freshwater flow of the Susquehanna River, and therefore has the highest concentrations of TSS and, due to washout, the lowest concentrations of chlorophyll. Chlorophyll concentrations peak at the mesohaline station, CB3.3C, and decline down estuary (Fig. 8b). Concentrations of TSS are minimal at the southernmost Maryland station, CB5.2, whereas concentrations of TSS at the York River (Virginia) polyhaline segment (YRKPH) showed more riverine characteristics, resembling the upper bay CB2.2 (Fig. 8c).

For all locations, coefficients of determination of the regressions used to determine specific-attenuation coefficients were lowest for K_d(PAR) than for any of the other quantities considered, and ranged from 0.87 to 0.98 (Table 5). Data characteristic of station CB5.2 produced the lowest r^2 (Table 5), due primarily to the low values and narrow range of TSS concentrations (Fig. 8b). The most variable coefficient was the intercept, K_w, with values ranging from 0.33 to 0.55 m^{-1}. The lowest occurred for

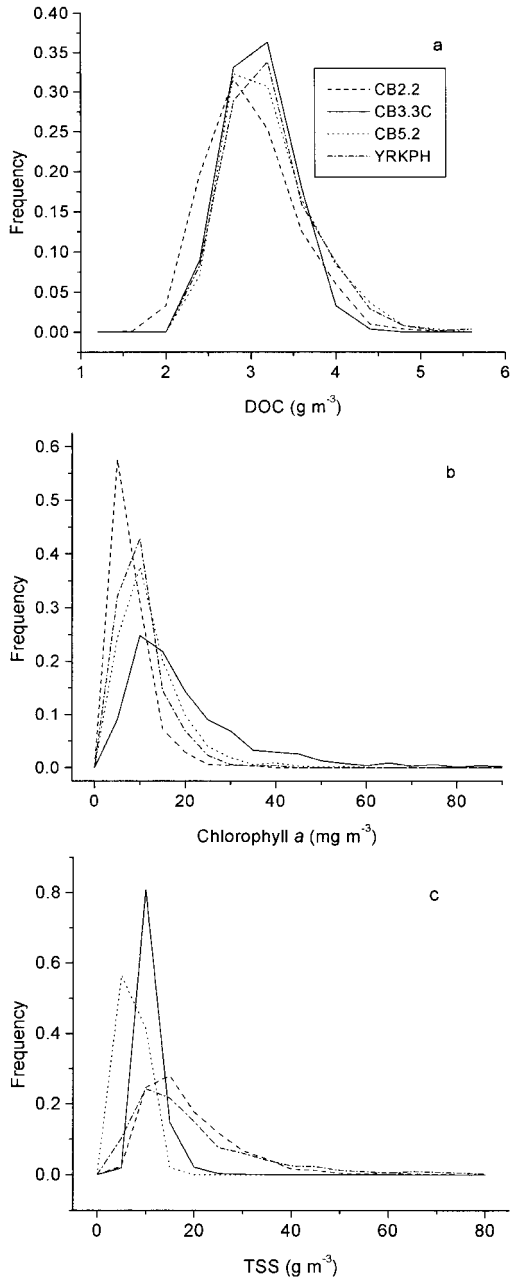

Fig. 8. Frequency distributions for optically important water quality parameters along a transect of stations in Chesapeake Bay, chosen to represent a range of salinity zones: CB2.2 = northern bay, oligohaline; CB3.3C = Chesapeake Bay Bridge, mesohaline; CB5.2 = Maryland-Virginia border, mesohaline; YRKPH = Mouth of York River, Virginia, polyhaline. Distributions are for (a) dissolved organic carbon (DOC), (b) phytoplankton chlorophyll, and (c) total suspended solids (TSS).

data with distributions resembling station CB5.2, and the highest for YRKPH and CB2.2, the 2 stations with the highest simulated concentrations of TSS (Fig. 8c). Also highly variable was the coefficient k_c, which ranged from 0.0122 to 0.0187 m^2 (mg chl *a*)$^{-1}$ (Table 5). The lowest value was produced by data characteristic CB3.3C, the station with the largest mean and widest range of chlorophyll concentrations.

Errors in Estimated Water Quality Targets

Variability in the specific-attenuation coefficients for PAR calculated from simulated error-free data gives cause to doubt whether the Lambert-Beer law can be applied reliably to PAR. This is important because it is measurements of PAR that are available to managers for determining water quality targets for SAV restoration. Noting that Eq. 6 is intended to describe the relationship between TSS and chlorophyll that maintains K_d(PAR) at a constant value, we can compare the linear representation with a set of ordered pairs of TSS and chlorophyll that maintain a constant K_d(PAR) determined numerically in the nonlinear SIAS model (Fig. 9a). For generating the numerically determined curves in Fig. 9a, the values of DOC and μ_0 were held constant at their mean values, and the solver routine in the spreadsheet software was used to obtain the value of TSS that gave the required K_d(PAR) for an array of assumed values of chlorophyll concentrations. Curves obtained in this way do not depend on application of the Lambert-Beer law, and require no a priori assumption about the shape of the minimum-light water quality requirement.

Two observations are apparent in this comparison. First, the minimum light requirements determined by the linear regressions differ substantially from those determined by numerical solution of the SIAS model (Fig. 9a). Minimum light requirements determined by linear regression are too lax for the 0.5-m and 1.0-m restoration depths, but indistinguishable for the 2-m restoration depths. This pattern results from failure of the Lambert-Beer law, as seen by the tendency of the linear regression to overestimate K_d(PAR) at K_d(PAR) < 1 m^{-1}, and to underestimate at K_d(PAR) $>$ about 1.5 m^{-1} (Fig. 7c). Second, even though the Lambert-Beer law has failed when applied across the complete range of K_d(PAR), curves of constant K_d(PAR) determined by numerical solution in the SIAS model (the bold lines in Fig. 9a) are nevertheless highly linear. This near linearity is maintained, in the case of the 0.5-m restoration depth, over a wide range of chlorophyll and TSS concentrations (Fig. 9a).

If we select the previously simulated data, in which [DOC] and μ_0 were allowed to vary, for a narrow range of K_d(PAR) such that $1.492 < K_d(\text{PAR}) < 1.537$ (i.e., percent of incident light at 1 m between 21.5 and 22.5), the points demonstrate scatter about the empirically determined

TABLE 5. Specific-attenuation coefficients determined from data simulated to match statistical distributions along a north-to-south transect along the mainstem Chesapeake Bay. Coefficients were estimated by linear regression of diffuse attenuation coefficient for PAR, K_d(PAR), against simulated concentrations of DOC (k_y), chlorophyll (k_c), and TSS (k_s). K_W = intercept of the regression. Units; k_y = m^2 (g DOC)$^{-1}$; k_c = m^2 (mg chl *a*)$^{-1}$; k_s = m^2 (g TSS)$^{-1}$; and K_W = m^{-1}. r^2 = coefficient of determination; SE = standard error of regression.

Station	K_W	k_y	k_c	k_s	r^2	SE
CB2.2	0.5483	0.0370	0.0187	0.0756	0.9595	0.1567
CB3.3C	0.3315	0.0507	0.0122	0.0778	0.9617	0.0725
CB5.2	0.3347	0.0504	0.0167	0.0954	0.8720	0.0970
YRKPH	0.5338	0.0503	0.0141	0.0737	0.9803	0.1800
Mean	0.4371	0.0471	0.0154	0.0806		
Std. dev.	0.1202	0.0067	0.0029	0.0100		
c.v. (%)	27.5	14.3	18.5	12.4		

line, but the additional variability reveals no systematic nonlinearity (Fig. 9b, circles). Most of the points selected in this way fall below the line determined by application of the regression (Fig. 9b, thin line). Selecting for a narrow range of $\mu_0 K_d$(PAR) (Fig. 9b, squares) indicates that much of the variability may be reduced by correction for the angle of incidence. The remaining scatter about the numerically-estimated minimum light requirement line is due to variability of DOC, and is non-systematic about the line established using the mean concentration.

An attempt to select data from the Chesapeake Bay Water Quality Monitoring Program (their station 3.3C) for a similarly narrow range of K_d(PAR) yielded 4 observations out of 180 records over a 10-yr period (Fig. 9b, plus signs). The observed data are both too sparse and too noisy to be useful for establishing minimum-light water quality requirements in Chesapeake Bay. The source of the noise in observed data will be examined elsewhere.

Failure of the Lambert-Beer law to apply to K_d(PAR) in Case 2 waters does not automatically invalidate the approach for obtaining SAV water quality targets outlined in Fig. 1. It does indicate that the minimum-light water quality requirements must be obtained empirically by separate application of an optical model for each restoration depth and fractional light requirement, rather than by application of a single regression equation. The revised procedure consists of estimating a slope, $\phi(Z_{max})$, and intercept, $S_0(Z_{max})$, in a linear relation between TSS and chlorophyll analogous to Eq. 6, i.e., $[TSS] = S_0(Z_{max}) - \phi(Z_{max})[Chl]$. The slope and intercept are estimated from the 'data' used to generate each of the bold lines in Fig. 9a.

Note that the coefficients in the regression depend explicitly on the restoration depth, and no longer depend explicitly on a unique set of specific-attenuation coefficients presumed to apply to all potential restoration depths (i.e., Eq. 6). This is not necessarily a disadvantage, since the applicability of the Lambert-Beer law (Eq. 4, from which Eq. 6 was derived) was in question from the outset. The value of Eq. 6 lies more in suggesting a potentially useful approach than it does in providing a mechanistic representation of the attenuation process. The SIAS model was shown here to be highly consistent with a fully mechanistic model of radiative transfer (Fig. 4). Therefore the minimum light water quality requirements generated from it should be as reliable as the specific-absorption and scattering spectra upon which it is based. Optical properties of the particulate material may be expected to vary with the source of the material, with spatial variations due to changing influence of freshwater versus marine particulates accounting for large, persistent differences in coefficients between regions. Coefficients S_0 and ϕ for both the 22% (mesohaline and polyhaline communities) and the 13% (oligohaline and tidal freshwater communities) light requirements are given in Table 6. Until a more comprehensive spatial analysis of optical properties is done, these coefficients must be based on the SIAS model calibrated for the Rhode River, Maryland, a tributary in the mesohaline zone of Chesapeake Bay. Determination of regionally customized coefficients has been identified as a high priority for restoration of SAV in the Chesapeake region (Moore et al. 2000). A spreadsheet for performing the calculations using coefficients determined here (Table 6) is available at www.chesapeakebay.net/cims/.

An Example Application

The Rhode River estuary, a tributary embayment on the western shore of Chesapeake Bay in Maryland, once had an abundant community of SAV (Southwick and Pine 1975) that disappeared through the decade of the 1970s. Specific-absorption and scattering spectra used in the SIAS model for calculating K_d(PAR) from water quality measurements were based on measurements in this system (Gallegos et al. 1990; Gallegos 1994).

Concentrations of suspended solids and phytoplankton chlorophyll have been monitored regu-

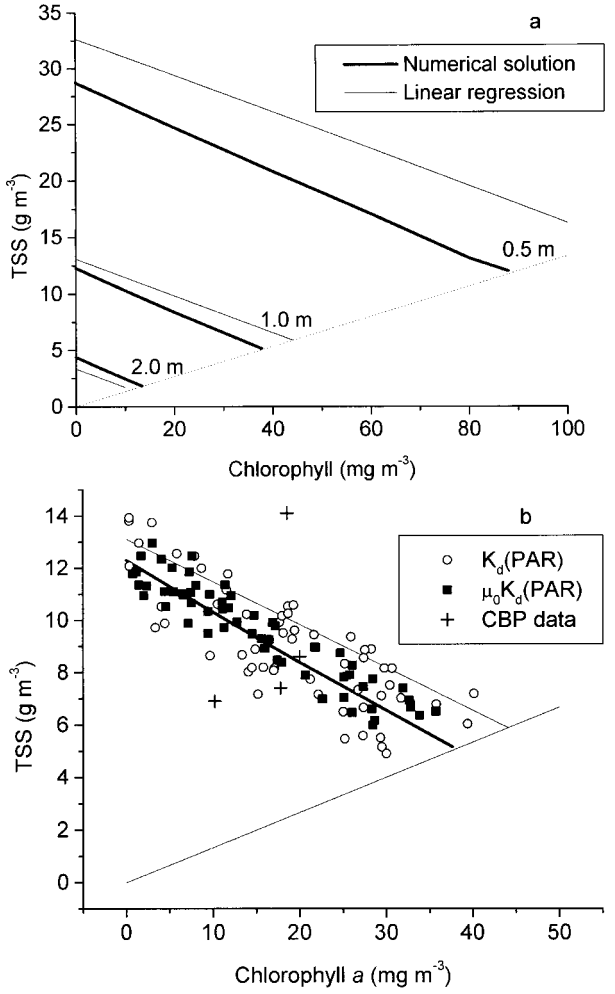

Fig. 9. a) Comparison of minimum-light water quality requirements calculated by (thin lines) application of Eq. 6 (derived by applying the Lambert-Beer law to the diffuse attenuation coefficient for PAR) with those calculated by numerical solution in the spreadsheet optical model, which does not require the assumption of the Lambert-Beer law. Numbers near lines give target restoration depths. Dotted line is approximate contribution of phytoplankton chlorophyll to total suspended solids (TSS). b) Effect of variability in simulated solar incidence angle and concentration of DOC on estimation of minimum-light water quality requirements for SAV growth to 1 m: open circles are concentrations of chlorophyll and TSS selected from the simulated data such that $1.492 \leq K_d(PAR) \leq 1.537$; filled squares are concentrations selected such that $1.238 \leq \mu_0 K_d \leq 1.276$ (i.e., median $\mu_0 = 0.83$). Correction for solar incidence angle reduces scatter about empirically calculated minimum-light water quality requirement. Data from the Chesapeake Bay Program (CBP) Water Quality Monitoring Program from station 3.3C selected for the same range of K_d (plus signs) yielded 4 observations, illustrating the difficulty in attempting to establish such limits from measured data. Bold and thin lines as in (a) are for 1 m restoration depth. Dotted line as in (a).

TABLE 6. Slope, ϕ, and intercept, S_0, in the regression of total suspended solids against chlorophyll concentration, that produce lines of constant diffuse attenuation coefficient, for meeting minimum light habitat requirements for growth of submersed aquatic vegetation to depths of 0.5, 1.0, and 2.0 m: $[TSS] = S_0 - \phi[Chl]$. Regression coefficients were determined as a linear fit to pairs of chlorophyll and suspended solids concentrations determined by numerical solution of the spreadsheet model of diffuse attenuation coefficient. Units of S_0 = g TSS m^{-3}; ϕ = g TSS (mg chl *a*)$^{-1}$. Thirteen percent light requirements are for tidal fresh and oligohaline areas; 22% light requirements are for mesohaline and polyhaline areas.

	13% Light Requirement		22% Light Requirement	
Z_{max}	S_0	ϕ	S_0	ϕ
0.5 m	41.054	0.1810	27.791	0.1874
1.0 m	17.949	0.1830	11.540	0.1905
2.0 m	6.595	0.1800	3.611	0.1908

larly since 1986. Annual growing season (April–October) medians of chlorophyll and TSS from 1986–1998 are plotted in relation to the 1 m minimum-light requirement line (Table 6) in Fig. 10. Ten of the 13 annual medians fail to meet the minimum-light requirement for growth to 1 m, as does the long-term median, given by $\mu_c = 23.43$ mg Chl m^{-3} and $\mu_s = 9.84$ g m^{-3} TSS (Fig. 10, asterisk). The target concentrations, calculated by substituting the values for the long-term medians into the formula in Table 7 for projection to origin, are 20.1

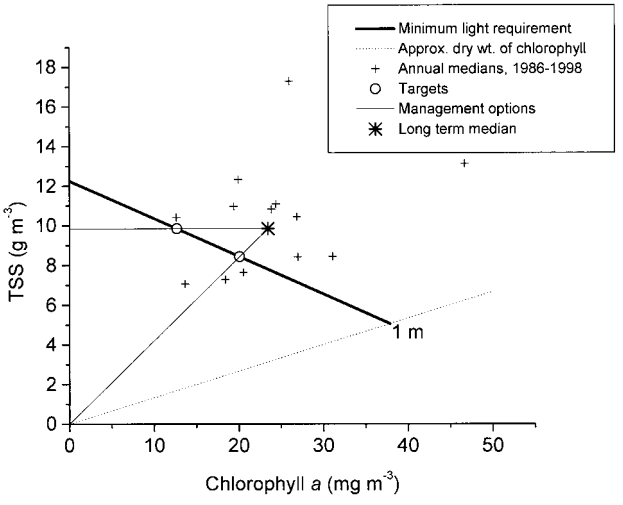

Fig. 10. Application of the water quality target estimation procedure to data from the Rhode River, Maryland. Minimum-light water quality requirement (bold line) was calculated empirically from the spectrally integrated model of diffuse attenuation. Target concentrations (open circles) of chlorophyll *a* and total suspended solids (TSS) are calculated as the intercept of the minimum-light water quality requirement with management options (thin lines) that would reduce (horizontal line) chlorophyll only or (diagonal line) chlorophyll and TSS from their current long term median concentrations (asterisk). Annual median concentrations (plus signs) are determined on data selected for SAV growing season; April through October.

TABLE 7. Formulae for coordinates of target concentrations of chlorophyll, [Chl], and total suspended solids, [TSS], determined by intersection of Eq. 7a–c with the linear fit to empirically determined pairs of [Chl] and [TSS] that meet SAV minimum light requirement using nonlinear optical model. Equation for the minimum light requirement is $[TSS] = S_0(Z_{max}) - \phi[Chl]$, where a separate estimate of intercept $[S_0(Z_{max})]$ and slope $[\phi(Z_{max})]$ are required for each restoration depth, Z_{max}. Dependence of coefficients on Z_{max} is omitted in the table for clarity. Last column gives conditions for obtaining a positive concentration as the intersection. μ_s = median concentration of TSS; μ_c = median concentration of chlorophyll *a*.

Management Action	[Chl]	[SPM]	Condition
Chlorophyll reduction only	$\frac{S_0 - \mu_s}{\phi}$	μ_s	$\mu_s \le S_0$
SPM reduction only	μ_c	$S_0 - \phi\mu_c$	$\mu_c \le \frac{S_0}{\phi}$
Projection to origin	$\frac{S_0\mu_c}{\phi\mu_c + \mu_s}$	$\frac{S_0\mu_s}{\phi\mu_c + \mu_s}$	No restrictions
Normal projection	$\frac{\phi S - \phi\mu_s + \mu_c}{1 + \phi^2}$	$\frac{S_0 + \phi^2\mu_s - \phi\mu_c}{1 + \phi^2}$	$\mu_s \le \frac{1}{\phi}\mu_c + S_0$ and $\mu_s \ge \frac{1}{\phi^2}(\phi\mu_c - S_0)$

mg chl m^{-3} and 8.4 g TSS m^{-3} (Fig. 10 circle). Managers would need to consider the relative controllability of chlorophyll (via nutrient reductions) versus TSS, much of which comes from in situ resuspension. A target based on chlorophyll reduction only, given by [Chl] = 12.66 mg m^{-3}, [TSS] = 9.84 g m^{-3}, may be the more attainable target (Fig. 10).

While it is true that SAV integrates environmental conditions (Dennison et al. 1993), short-term events can also affect growth and survival of SAV. For example, Moore et al. (1997) documented the impact of a month-long turbidity pulse on the demise of transplanted eelgrass beds at an upriver site in the York River, Virginia. The losses occurred even though annual median daily attenuation coefficients were not statistically different from those at a downriver site where the turbidity pulse was not as evident and grasses survived. Two similar events are identifiable in the Rhode River data (Fig. 10). A late spring freshet in 1989 (Gallegos et al. 1992) caused high growing season chlorophyll concentrations (median $>$ 45 mg m^{-3}), and the spring storm of March 1993 produced near record flows of the Susquehanna River and high suspended solids concentrations (median TSS $>$ 17 g m^{-3}). It is possible that the calculation of water quality concentrations from measured data needs to be weighted for timing in relation to critical growth stages. Duration of low-light events may also be a factor (Moore et al. 1997 and references therein). The weights assigned to different time periods would vary with the growth characteristics of different SAV species, but procedures for calculating water quality targets from suitably weighted averages would remain unchanged.

Summary and Conclusions

A simplified procedure for calculating minimum-light water quality goals for protection and restoration of SAV is presented, based on application of the Lambert-Beer law to the diffuse attenuation coefficient for downwelling photosynthetically active radiation, K_d(PAR). The applicability of the Lambert-Beer law in Case 2 waters in general and to PAR in particular was investigated using a simple spectrally integrated algebraic summary (SIAS) model of diffuse attenuation based on the equation of Kirk (1984, Eq. 2). The SIAS model was shown to predict values of diffuse attenuation coefficient for both spectral irradiance and PAR that agreed very well with those determined by Monte Carlo simulation of the radiative transfer equations (Fig. 4).

The SIAS model was used to simulate spectral and broadband diffuse attenuation coefficients in Case 2 waters with conditions typical of mesohaline mainstem Chesapeake Bay (Fig. 5). With application of the simple correction for geometry of the underwater light field proposed by Gordon (1989), diffuse attenuation coefficient obeyed the Lambert-Beer to within about 8% (Fig. 7b,d). Without correction, errors associated with estimating K_d from a linear regression on water quality concentrations were about 14% for narrow and broadband K_d (Fig. 7a,c). Errors in estimated K_d(PAR) varied asymmetrically, resulting in mostly overestimates at low K_d(PAR) and underestimates at intermediate and high K_d(PAR) (Fig. 7c). The tendency toward asymmetric errors caused the calculated minimum-light water quality lines (lines of constant K_d(PAR) as a function of TSS and chlorophyll) to diverge from those determined by nu-

merical solution of the SIAS model (Fig. 9a). These errors in calculated minimum-light water quality criteria were a direct result of failure of K_d(PAR) to obey the Lambert-Beer law.

In spite of the failure of K_d(PAR) to conform to the Lambert-Beer law across a wide range of K_d, the numerically determined minimum-light water quality targets were linear to a very high degree (Fig. 9). Even though K_d(PAR) is not a linear function of the optical water quality concentrations, at constant K_d, the covariation of TSS and chlorophyll is very nearly linear (Fig. 9). The procedure of determining water quality goals from the intersection of lines describing the variation of water quality concentrations at constant K_d(PAR) and a water quality improvement strategy remains valid (Fig. 10), even though the coefficients in the line describing the minimum-light water quality requirements must be determined empirically by application of a suitably calibrated optical model.

The revised procedure meets the dual (and potentially conflicting) requirements for accuracy and ease of use for managers. Accuracy is assured because the model used to generate the minimum-light water quality requirements has now been validated against more mechanistic simulations of the radiative transfer equations. The procedure is easy to use because large amounts of data can be displayed in 2 dimensions, and water quality targets calculated analytically and automatically. Widespread application of the procedure will require that we gain a better understanding of the regional variability in specific-absorption and scattering spectra of particulate matter. As will be shown in a related paper, this requirement would have been necessary even if K_d(PAR) had conformed to the Lambert-Beer, due to difficulties in estimating specific-attenuation coefficients from large scale water quality monitoring programs with very limited optical data.

Acknowledgments

Measurements used to estimate specific-absorption and scattering coefficients of TSS were funded by the Estuarine Habitat Program of the Coastal Ocean Program, National Oceanic and Atmospheric Administration. Data for application of the diagnostic tool to the Rhode River were provided by the Smithsonian Environmental Sciences Program and made available by Tom Jordan. I am especially grateful John T. O. Kirk for kindly supplying the code for his Monte Carlo model and to Richard Batiuk for his leadership of the SAV Technical Synthesis-2 authorship team.

Literature Cited

Batiuk, R. A., R. J. Orth, K. A. Moore, W. C. Dennison, J. C. Stevenson, L. Staver, V. Carter, N. Rybicki, R. E. Hickman, S. Kollar, S. Bieber, P. Heasly, and P. Bergstrom. 1992. Chesapeake Bay Submerged Aquatic Vegetation Habitat Requirements and Restoration Goals: A Technical Synthesis. U.S. Environmental Protection Agency, Chesapeake Bay Program, Annapolis, Maryland.

Carter, V., N. B. Rybicki, J. M. Landwehr, and M. Naylor. 2000. Light requirements for SAV survival and growth, p. 4–15. *In* R. A. Batiuk, P. Bergstrom, W. M. Kemp, E. Koch, L. Murray, J. C. Stevenson, R. Bartleson, V. Carter, N. B. Rybicki, J. M. Landwehr, C. Gallegos, L. Karrh, M. Naylor, D. Wilcox, K. A. Moore, S. Ailstock, and M. Teichberg (eds.), Chesapeake Bay Submerged Aquatic Vegetation Water Quality and Habitat-based Requirements and Restoration Targets: A Second Technical Synthesis. U.S. Environmental Protection Agency, Chesapeake Bay Program, Annapolis, Maryland.

Davies-Colley, R. J., W. N. Vant, and D. G. Smith. 1993. Colour and Clarity of Natural Waters. Ellis Horwood, Chichester.

Dennison, W. C., R. J. Orth, K. A. Moore, J. C. Stevenson, V. Carter, S. Kollar, P. W. Bergstrom, and R. A. Batiuk. 1993. Assessing water quality with submersed aquatic vegetation. *BioScience* 43:86–94.

Duarte, C. M. 1991. Seagrass depth limits. *Aquatic Botany* 40: 363–377.

Gallegos, C. L. 1994. Refining habitat requirements of submersed aquatic vegetation: Role of optical models. *Estuaries* 17:198–219.

Gallegos, C. L., D. L. Correll, and J. W. Pierce. 1990. Modeling spectral diffuse attenuation, absorption, and scattering coefficients in a turbid estuary. *Limnology and Oceanography* 35: 1486–1502.

Gallegos, C. L., T. E. Jordan, and D. L. Correll. 1992. Event-scale response of phytoplankton to watershed inputs in a subestuary: Timing, magnitude, and location of phytoplankton blooms. *Limnology and Oceanography* 37:813–828.

Gallegos, C. L. and W. J. Kenworthy. 1996. Seagrass depth limits in the Indian River Lagoon (Florida, U.S.A.): Application of an optical water quality model. *Estuarine, Coastal and Shelf Science* 42:267–288.

Gallegos, C. and K. A. Moore. 2000. Factors contributing to water-column light attenuation, p. 16–27. *In* R. A. Batiuk, P. Bergstrom, W. M. Kemp, E. Koch, L. Murray, J. C. Stevenson, R. Bartleson, V. Carter, N. B. Rybicki, J. M. Landwehr, C. Gallegos, L. Karrh, M. Naylor, D. Wilcox, K. A. Moore, S. Ailstock, and M. Teichberg (eds.), Chesapeake Bay Submerged Aquatic Vegetation Water Quality and Habitat-based Requirements and Restoration Targets: A Second Technical Synthesis. U.S. Environmental Protection Agency, Chesapeake Bay Program, Annapolis, Maryland.

Geider, R. J. 1987. Light and temperature dependence of the carbon to chlorophyll *a* ratio in microalgae and cyanobacteria: Implications for physiology and growth of phytoplankton. *New Phytologist* 106:1–34.

Gordon, H. R. 1989. Can the Lambert-Beer law be applied to the diffuse attenuation coefficient of ocean water? *Limnology and Oceanography* 34:1389–1409.

Kemp, W. M., R. Bartleson, and L. Murray. 2000. Epiphyte contributions to light attenuation at the leaf surface, p. 28–37. *In* R. A. Batiuk, P. Bergstrom, W. M. Kemp, E. Koch, L. Murray, J. C. Stevenson, R. Bartleson, V. Carter, N. B. Rybicki, J. M. Landwehr, C. Gallegos, L. Karrh, M. Naylor, D. Wilcox, K. A. Moore, S. Ailstock, and M. Teichberg (eds.), Chesapeake Bay Submerged Aquatic Vegetation Water Quality and Habitat-based Requirements and Restoration Targets: A Second Technical Synthesis. U.S. Environmental Protection Agency, Chesapeake Bay Program, Annapolis, Maryland.

Kirk, J. T. O. 1980. Relationship between nephelometric turbidity and scattering coefficients in certain Australian waters. *Australian Journal of Marine and Freshwater Research* 31:1–12.

Kirk, J. T. O. 1981. Monte Carlo study of the nature of the underwater light field in, and the relationships between optical properties of, turbid, yellow waters. *Australian Journal of Marine and Freshwater Research* 32:517–532.

KIRK, J. T. O. 1984. Dependence of relationship between apparent and inherent optical properties of water on solar altitude. *Limnology and Oceanography* 29:350–356.

KIRK, J. T. O. 1989. The upwelling light stream in natural waters. *Limnology and Oceanography* 34:1410–1425.

KIRK, J. T. O. 1994. Light and Photosynthesis in Aquatic Ecosystems. Cambridge University Press, Cambridge.

KOCH, E. W. 2001. Beyond light: Physical, geological and geochemical parameters as possible submerged aquatic vegetation habitat requirements. *Estuaries* 24:1–17.

LORENZEN, C. J. 1972. Extinction of light in the ocean by phytoplankton. *Journal du Conseil, Conseil International pour l'Exploration de la Mer* 34:262–267.

MOBLEY, C. D. 1994. Light and Water. Radiative Transfer in Natural Waters. Academic Press, New York.

MOBLEY, C. D., B. GENTILI, H. R. GORDON, Z. JIN, G. W. KATTAWAR, A. MOREL, P. REINERSMAN, K. STAMNES, AND R. H. STAVN. 1993. Comparison of numerical models for computing underwater light fields. *Applied Optics* 32:1–21.

MOORE, K. A., W. M. KEMP, V. CARTER, AND C. GALLEGOS. 2000. Future needs for continued management application, p. 77–78. *In* R. A. Batiuk, P. Bergstrom, W. M. Kemp, E. Koch, L. Murray, J. C. Stevenson, R. Bartleson, V. Carter, N. B. Rybicki, J. M. Landwehr, C. Gallegos, L. Karrh, M. Naylor, D. Wilcox, K. A. Moore, S. Ailstock, and M. Teichberg (eds.), Chesapeake Bay Submerged Aquatic Vegetation Water Quality and Habitat-based Requirements and Restoration Targets: A Second Technical Synthesis. U.S. Environmental Protection Agency, Chesapeake Bay Program, Annapolis, Maryland.

MOORE, K. A., R. L. WETZEL, AND R. J. ORTH. 1997. Seasonal pulses of turbidity and their relations to eelgrass (*Zostera marina* L.) survival in an estuary. *Journal of Experimental Marine Biology and Ecology* 215:115–134.

MOREL, A. AND B. GENTILI. 1991. Diffuse reflectance of oceanic waters: Its dependence on sun angle as influenced by the molecular scattering contribution. *Applied Optics* 30:4427–4438.

MOREL, A. AND R. C. SMITH. 1982. Terminology and units in optical oceanography. *Marine Geodesy* 5:335–349.

ORTH, R. J. AND K. A. MOORE. 1983. Chesapeake Bay: An unprecedented decline in submerged aquatic vegetation. *Science* 222:51–53.

SMITH, JR., W. O. 1982. The relative importance of chlorophyll, dissolved and particulate material, and seawater to the vertical extinction of light. *Estuarine, Coastal and Shelf Science* 15:459–465.

SOUTHWICK, C. H. AND F. W. PINE. 1975. Abundance of submerged vascular vegetation in the Rhode River from 1966 to 1973. *Chesapeake Science* 16:147–151.

STEFAN, H. G., J. J. CARDONI, F. R. SCHIEBE, AND C. M. COOPER. 1983. Model of light penetration in a turbid lake. *Water Resources Research* 19:109–120.

SVERDRUP, H. U., M. W. JOHNSON, AND R. H. FLEMING. 1942. The Oceans, Their Physics, Chemistry, and General Biology. Prentice-Hall, Englewood Cliffs.

TWILLEY, R. R., W. M. KEMP, K. W. STAVER, J. C. STEVENSON, AND W. R. BOYNTON. 1985. Nutrient enrichment of estuarine submersed vascular plant communities. 1. Algal growth and effects on production of plants and associated communities. *Marine Ecology Progress Series* 23:179–191.

VANT, W. N. 1990. Causes of light attenuation in nine New Zealand estuaries. *Estuarine, Coastal and Shelf Science* 31:125–137.

VERDUIN, J. 1982. Components contributing to light extinction in natural waters: Method of isolation. *Archiv für Hydrobiologie* 93:303–312.

WEIDEMANN, A. D. AND T. T. BANNISTER. 1986. Absorption and scattering coefficients in Irondequoit Bay. *Limnology and Oceanography* 31:567–583.

Received for consideration, March 13, 2000
Accepted for publication, December 6, 2000